

# The Lie-Group Shooting Method for Thermal Stress Evaluation Through an Internal Temperature Measurement

Chein-Shan Liu<sup>1</sup>

**Abstract:** In the present work we study numerical computations of inverse thermal stress problems. The unknown boundary conditions of an elastically deformable heat conducting rod are not given a priori and are not allowed to measure directly, because the boundary may be not accessible to measure. However, an internal measurement of temperature is available. We treat this inverse problem by using a semi-discretization technique, of which the time domain is divided into many sub-intervals and the physical quantities are discretized at these node points of discrete times. Then the resulting ordinary differential equations in the discretized space are numerically integrated towards the spatial direction by the Lie-group shooting method to find unknown boundary conditions. The key point is based on one-step Lie group elements:  $\mathbf{G}(r) = \mathbf{G}(\mathbf{y}^0, \mathbf{y}^\ell)$ . We are able to search missing boundary conditions through a minimum discrepancy from the targets in terms of a weighting factor  $r \in (0, 1)$ . Several numerical examples were worked out to persuade that this novel approach has good efficiency and accuracy. Although the measured temperature is disturbed by large noise, the Lie group shooting method is stable to recover the boundary conditions very well.

**Keyword:** Inverse problem, Inverse thermal stress problem, Lie-group shooting method, Group preserving scheme

## 1 Introduction

Recently, thermally induced stress analyses with heat transfer for several geometries and boundary

conditions have been solved numerically by many researches, for example, Chen and Liu (2001), Miyazaki, Tamura and Yamamoto (2000), and Gulluoglu and Tsai (2000). Al-Huniti, Al-Nimr and Naji (2001) have investigated the dynamic thermal and elastic behavior of a rod due to a moving heat source. They used an analytical-numerical technique based on the Laplace transformation and the Riemann-sum approximation to calculate the temperature, displacement and stress distributions in the rod. By using the Laplace transform method, Grysa, Cialkowski and Kaminski (1981) have applied the thermal stress theory to investigate the inverse problem of finding temperature and stress fields from the measurements of temperature, heat flux and displacement at some points inside the solid. In order to obtain a more accurate estimated result, the measurement location should be located near the position of unknown boundary condition. In addition, their estimated results were also sensitive to the internal measurement errors and the magnitude of time step. Blanc and Raynaud (1996) have estimated unknown boundary condition of an inverse problem by using the thermal strain and temperature measurements instead of the temperature measurements only.

For the inverse heat conduction problem (IHCP) it is well known that the numerical schemes are easily sensitive to measurement noises. In order to overcome this drawback, Chen and Chang (1990) have introduced a hybrid scheme of the Laplace transform and finite-difference methods to estimate unknown surface temperature in an one-dimensional IHCP using the measured temperatures inside the material without measurement errors. Similarly, the measurement location was better located near the position of unknown boundary condition in order to obtain a more ac-

---

<sup>1</sup>Department of Mechanical & Mechatronic Engineering and Department of Harbor & River Engineering, Taiwan Ocean University, Keelung, Taiwan. E-mail: csliau@mail.ntou.edu.tw

curate estimated result. Recently, a large improvement to overcome the above drawback has been made by Chen, Lin and Fang (2001, 2002), who applied a similar scheme in conjunction with a sequential-in-time concept and the least-squares method to estimate unknown surface condition from the temperature measurements. Then, Chen, Wu and Hsiao (2004) have studied by applying the same technique to predict unknown surface condition from the theory of dynamic thermal stress. The results of their study show that a good estimation can be obtained even for the case with measurement errors.

Chang, Liu and Chang (2005) have solved the IHCP of boundary condition identification by using the group preserving scheme (GPS). A rather comprehensive review of different techniques to solve the IHCP has been surveyed in that paper. We are going to extend it to the inverse thermal stress problem (ITSP), of which stress is calculated by the following constitutive equation:

$$\sigma(x, t) = \frac{2G}{1-2\nu} \left[ (1-\nu) \frac{\partial u(x, t)}{\partial x} - (1+\nu) \alpha_t T(x, t) \right], \quad (1)$$

where  $t$  is the time,  $x$  is the spatial coordinate,  $\nu$  is the Poisson ratio and  $\alpha_t$  is the coefficient of thermal expansion.

The linear momentum balance equation is written as

$$\frac{\partial \sigma(x, t)}{\partial x} = \rho \frac{\partial^2 u(x, t)}{\partial t^2}, \quad (2)$$

where  $\rho$  is the material density. Substituting Eq. (1) into Eq. (2) we obtain

$$\frac{\partial^2 u(x, t)}{\partial x^2} - \frac{1}{c^2} \frac{\partial^2 u(x, t)}{\partial t^2} = k \frac{\partial T(x, t)}{\partial x}, \quad 0 < x < \ell, \quad 0 < t \leq t_f, \quad (3)$$

where  $t_f$  is a final time,  $\ell$  is the length of rod, and the coefficients are defined as

$$c = \sqrt{\frac{2G(1-\nu)}{\rho(1-2\nu)}}, \quad k = \frac{(1+\nu)\alpha_t}{1-\nu}. \quad (4)$$

The one-dimensional heat conduction equation with constant thermal properties can be expressed as

$$\frac{\partial^2 T(x, t)}{\partial x^2} = \frac{1}{\alpha} \frac{\partial T(x, t)}{\partial t}, \quad 0 < x < \ell, \quad 0 < t \leq t_f, \quad (5)$$

where  $\alpha$  is the thermal diffusivity.

The present ITSP is subjected to the following boundary conditions:

$$T_x(0, t) = 0, \quad T(\ell, t) = F_\ell(t), \quad (6)$$

$$u(0, t) = 0, \quad \sigma(\ell, t) = 0, \quad (7)$$

and initial conditions:

$$T(x, 0) = f(x), \quad u(x, 0) = g(x), \quad u_t(x, 0) = h(x). \quad (8)$$

However,  $F_\ell(t)$  is an unknown function. This point is different from the direct problem, where  $F_\ell(t)$  is given. For the inverse problem,  $F_\ell(t)$  can be estimated, provided that the internal measurement of temperature at an internal point  $x = x_m$  is available:

$$T(x_m, t) = F_m(t). \quad (9)$$

When it is impossible to measure the temperature on an inaccessible surface directly, such as in the use of combustion chambers, nuclear reactors, heat exchangers and re-entry vehicles, etc., the ITSP is often occurred in engineering appliances, in which one wants to resolve the surface temperature from measurements inside a heat-conducting object. The problem setup with its physical model is shown in Fig. 1. The purpose of the present paper is using the above equations to recover the thermal stress, displacement and temperature of an elastically deformable heat conducting rod. Moreover, in a practical use we are usually required to mount a thermocouple as far away from the surface as possible for not destroying the structure of the engineering appliance too much, which means that  $x_m$  should be much smaller than  $\ell$ .

The main difficulties of the ITSP are that for Eq. (5) there has an unknown boundary condition

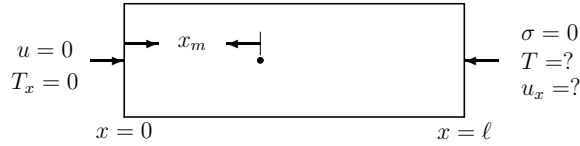


Figure 1: A schematic diagram of the inverse thermal stress problem.

$T(\ell, t) = F_\ell(t)$  in Eq. (6), and that when  $T(x, t)$  is not available in the whole spacetime domain we have to solve Eq. (3), of which  $T_x(x, t)$  is as a source term and there is also an unknown Neumann boundary condition for  $u$  specified by

$$u_x(\ell, t) = kT(\ell, t) = kF_\ell(t). \quad (10)$$

Due to these difficulties, in the past studies the measurement point is necessarily located near the position of unknown boundary condition in order to obtain a more accurate estimated result. On the other hand, in the paper by Chen, Wu and Hsiao (2004) the measurement point  $x_m$  in Eq. (9) is located at the left-boundary. From this condition together with the condition  $T_x(0, t) = 0$  in Eq. (6), one really has a direct problem (not an IHCP) to solve Eq. (5) by integrating it in the  $x$ -direction. Then, it is not difficult to obtain the whole temperature in the rod and moreover the condition (10) can be available. Hence, we can treat the wave equation (3) by using a general method for direct problem to find the displacement and then the thermal stress in Eq. (1). In this regard the problem treated by Chen, Wu and Hsiao (2004) under the condition of  $x_m = 0$  is not an inverse problem, even they claimed that it is an inverse thermal stress problem.

Here we are attempting to develop a new Lie-group shooting method (LGSM) for the ITSP. It is an extension of the works by Liu (2004), Liu, Chang and Chang (2006a) and Chang, Liu and Chang (2007a). Recently, Liu (2008a, 2008b) has explored its superiority by using the LGSM to estimate parameters in parabolic type PDEs.

The ITSP is one of the inverse problems for the applications in heat conduction engineering by considering thermal stress. The inverse problems are those in which one would determine

the causes for an observed effect. One of the characterizing properties of many of the inverse problems is that they are usually ill-posed, in the sense that a solution that depends continuously on the data does not exist. For the present ITSP the observed effect is the temperature measurement  $T(x_m, t)$  made at an internal point  $x = x_m$  in the rod. We are interesting to search the causes of these two unknown boundary conditions in Eqs. (6) and (10), which induce the effect we observe through measurement. For the inverse problems the measurement error may often lead to a large discrepancy of the causes.

The LGSM is originally used for the boundary value problems as designed by Liu (2006a, 2006b, 2006c) for direct problems. However, these methods are restricted only for the two-dimensional ordinary differential equations (ODEs), and here we will extend them to the multi-dimensional problems. In a series of papers by the author and his coworkers, the Lie group shooting method reveals its excellent behavior on the numerical solutions of different boundary value problems, for example, Chang, Chang and Liu (2006, 2008) and Liu and Chang (2008) to treat the boundary layer equations in fluid mechanics, Liu, Chang and Chang (2006b) to treat the Burgers equation, Chang, Liu and Chang (2007a, 2007b) to treat the backward heat conduction equation, and Liu (2008c) to treat an inverse Sturm-Liouville problem.

It is interesting to note that the new method of LGSM does not require any a priori regularization when applying it to the ITSP, and also exhibits several advantages than other methods. It would be clear that the new method can greatly reduce the computational time and is very easy to implement on the calculations of ITSP. Especially, when the thermocouple is mounted in a position far away from the surface of unknown boundary conditions for a safety reason, the present method of LGSM would provide much better computational results than others, which in turns greatly suggest us to use the LGSM in these calculations of ITSP when  $x_m$  is limited to be small for a safety reason.

## 2 Numerical solution procedures

We are going to solve the ITSP through three steps. First, we use the Lie-group shooting method to solve the heat conduction problem in a spatial interval of  $0 < x < x_m$  by subjecting to the initial condition, the Neumann boundary condition at the left-side  $x = 0$  and an available measured data at the right-side  $x = x_m$ . The numerical procedures and numerical examples will be exposed in Section 6.

Then the above solution is extended into the whole domain in the interval of  $0 < x < \ell$ , which is substituted into Eq. (3) providing a right-hand side function. We transform Eq. (3) into the following equations:

$$\frac{\partial u(x,t)}{\partial x} = v(x,t), \quad (11)$$

$$\frac{\partial v(x,t)}{\partial x} = \frac{1}{c^2} \frac{\partial^2 u(x,t)}{\partial t^2} + k \frac{\partial T(x,t)}{\partial x}. \quad (12)$$

Then, in the third step, by using a semi-discretization method to discretize the quantities of  $u(x,t)$  and  $v(x,t)$  along the time direction, we can obtain a system of ODEs for  $u$  and  $v$  with  $x$  as an independent variable. The Lie group shooting method as developed by Liu (2006a) is thus extended and applied to the following discretized equations:

$$\frac{\partial u^i(x)}{\partial x} = v^i(x), \quad i = 2, \dots, n, \quad (13)$$

$$\frac{\partial v^i(x)}{\partial x} = \left[ \frac{u^{i+1}(x) - 2u^i(x) + u^{i-1}(x)}{c^2(\Delta t)^2} + k \frac{\partial T(x, t_i)}{\partial x} \right], \quad i = 2, \dots, n, \quad (14)$$

where  $u^i(x) = u(x, i\Delta t)$  and  $v^i(x) = v(x, i\Delta t)$  and  $\Delta t = t_f/n$  is a uniform discretization time increment. The two known boundary conditions are given by

$$u^i(0) = 0, \quad i = 2, \dots, n, \quad (15)$$

$$v^i(\ell) = kT(\ell, t_i), \quad i = 2, \dots, n, \quad (16)$$

which are obtained from Eq. (7).

In Eq. (14), the unknown function  $u^{n+1}(x)$  is set equal to zero. On the other hand, according to the

finite difference and initial conditions which are specified for both  $u^0(x) = u(x, 0)$  and  $u_t(x, 0)$  we can obtain

$$u^1(x) = u^0(x) + u_t(x, 0)\Delta t, \quad (17)$$

where the value of  $u^0(x) = u(x, 0)$  is determined by the initial condition. It means that  $u^1(x)$  is fully determined by these two initial conditions  $g(x)$  and  $h(x)$  in Eq. (8), and at the same time  $v^1(x)$  is determined by  $v^1(x) = \partial u^1(x)/\partial x$ . Therefore, the two variables  $u^1(x)$  and  $v^1(x)$  in Eqs. (13) and (14) should be deemed as known functions. This is the reason that we let  $i$  start from  $i = 2$  in the above equations.

Obviously, there are two missing boundary conditions  $u^i(\ell)$ ,  $i = 2, \dots, n$  and  $v^i(0)$ ,  $i = 2, \dots, n$  in Eqs. (13) and (14). In Section 4 we will use the LGSM to calculate these quantities. Upon the left-boundary condition of  $v^i$  is obtained, we can treat Eqs. (13) and (14) as a coupled ODEs system supplemented with a source term  $T(x, t_i)$ , which is already calculated in the first step, and we can use the GPS or other available numerical integrators to calculate  $u^i$  and  $v^i$ . If both  $u(x, t)$  and  $T(x, t)$  are available, we can use Eq. (1) to calculate stress  $\sigma(x, t)$ .

## 3 Mathematical preliminaries

### 3.1 The GPS

Let us write Eqs. (13) and (14) as in a vector form:

$$\mathbf{y}' = \mathbf{f}(x, \mathbf{y}), \quad (18)$$

where the prime denotes the differential with respect to  $x$ , and

$$\mathbf{y} := \begin{bmatrix} \mathbf{y}_1 \\ \mathbf{y}_2 \end{bmatrix}, \quad \mathbf{f} := \begin{bmatrix} \mathbf{y}_2 \\ \mathbf{h}(x, \mathbf{y}_1) \end{bmatrix}, \quad (19)$$

in which  $\mathbf{y}_1 = (u^2, \dots, u^n)^t$  and  $\mathbf{y}_2 = (v^2, \dots, v^n)^t$ . Each component of  $\mathbf{h}$  represents the right-hand side of Eq. (14).

Liu (2001) has embedded Eq. (18) into an aug-

mented system:

$$\begin{aligned} \mathbf{X}' &:= \frac{d}{dx} \begin{bmatrix} \mathbf{y} \\ \|\mathbf{y}\| \end{bmatrix} \\ &= \begin{bmatrix} \mathbf{0}_{(2n-2) \times (2n-2)} & \frac{\mathbf{f}(x, \mathbf{y})}{\|\mathbf{y}\|} \\ \frac{\mathbf{f}(x, \mathbf{y})}{\|\mathbf{y}\|} & 0 \end{bmatrix} \begin{bmatrix} \mathbf{y} \\ \|\mathbf{y}\| \end{bmatrix} \quad (20) \\ &:= \mathbf{A}\mathbf{X}, \end{aligned}$$

where  $\|\mathbf{y}\|$  denotes the Euclidean norm of  $\mathbf{y}$ , and  $\mathbf{A}$  is an element of the Lie algebra  $so(2n-2, 1)$  satisfying

$$\mathbf{A}^t \mathbf{g} + \mathbf{g}\mathbf{A} = \mathbf{0} \quad (21)$$

with

$$\mathbf{g} = \begin{bmatrix} \mathbf{I}_{2n-2} & \mathbf{0}_{(2n-2) \times 1} \\ \mathbf{0}_{1 \times (2n-2)} & -1 \end{bmatrix} \quad (22)$$

a Minkowski metric. Here,  $\mathbf{I}_{2n-2}$  is the identity matrix, and the superscript  $t$  stands for the transpose.

The augmented variable  $\mathbf{X}$  satisfies the cone condition:

$$\mathbf{X}^t \mathbf{g} \mathbf{X} = \mathbf{y} \cdot \mathbf{y} - \|\mathbf{y}\|^2 = 0. \quad (23)$$

Accordingly, Liu (2001) has developed a group preserving scheme (GPS) to guarantee that each  $\mathbf{X}_k$  locates on the cone:

$$\mathbf{X}_{k+1} = \mathbf{G}(k)\mathbf{X}_k, \quad (24)$$

where  $\mathbf{X}_k$  denotes the numerical value of  $\mathbf{X}$  at the discretized point  $x_k$ , and  $\mathbf{G}(k) \in SO_o(2n-2, 1)$  satisfies

$$\mathbf{G}^t \mathbf{g} \mathbf{G} = \mathbf{g}, \quad (25)$$

$$\det \mathbf{G} = 1, \quad (26)$$

$$G_0^0 > 0, \quad (27)$$

where  $G_0^0$  is the 00th component of  $\mathbf{G}$ .

### 3.2 One-step Lie-group transformation

Applying scheme (24) to Eq. (20) with a specified condition  $\mathbf{X}(0) = \mathbf{X}^0$  we can compute the solution  $\mathbf{X}(x)$  by the GPS. Assuming that the stepsize used in the GPS is  $\Delta x = \ell/K$ , and starting from an

augmented condition  $\mathbf{X}^0 = ((\mathbf{y}^0)^t, \|\mathbf{y}^0\|)^t$  we will calculate the value  $\mathbf{X}^\ell = ((\mathbf{y}^\ell)^t, \|\mathbf{y}^\ell\|)^t$  at  $x = \ell$ .

By applying Eq. (24) step-by-step we can obtain

$$\mathbf{X}^\ell = \mathbf{G}_K(\Delta x) \cdots \mathbf{G}_1(\Delta x) \mathbf{X}^0. \quad (28)$$

However, let us recall that each  $\mathbf{G}_i$ ,  $i = 1, \dots, K$ , is an element of the Lie group  $SO_o(2n-2, 1)$ , and by the closure property of Lie groups,  $\mathbf{G}_K(\Delta x) \cdots \mathbf{G}_1(\Delta x)$  is also a Lie group denoted by  $\mathbf{G}$ . Hence, we have

$$\mathbf{X}^\ell = \mathbf{G}\mathbf{X}^0. \quad (29)$$

This is a one-step transformation from  $\mathbf{X}^0$  to  $\mathbf{X}^\ell$ .

It should be stressed that the one-step Lie-group transformation property is obviously not shared by other numerical methods, when those methods do not belong to the Lie-group types. This important behavior has first pointed out by Liu (2006d) and used to solve the backward in time Burgers equation. After that Liu (2006e) has used this concept to establish a one-step estimation method to estimate the temperature-dependent thermal conductivity, and then extended to estimate thermophysical properties [Liu (2006f); Liu (2007); Liu, Liu and Hong (2007)].

### 3.3 Generalized mid-point method

The remaining problem is how to calculate  $\mathbf{G}$ . While an exact calculation of  $\mathbf{G}$  is difficult, we can calculate  $\mathbf{G}$  by a generalized mid-point method, which is obtained from an exponential mapping of  $\mathbf{A}$  by taking the values of the argument variables of  $\mathbf{A}$  at a generalized mid-point. The Lie group generated from  $\mathbf{A} \in so(2n-2, 1)$  by an exponential admits a closed-form representation given as follows:

$$\mathbf{G} = \begin{bmatrix} \mathbf{I}_{2n-2} + \frac{(a-1)\hat{\mathbf{f}}\hat{\mathbf{f}}}{\|\hat{\mathbf{f}}\|^2} & \frac{b\hat{\mathbf{f}}}{\|\hat{\mathbf{f}}\|} \\ \frac{b\hat{\mathbf{f}}}{\|\hat{\mathbf{f}}\|} & a \end{bmatrix}, \quad (30)$$

where

$$\hat{\mathbf{y}} = r\mathbf{y}^0 + (1-r)\mathbf{y}^\ell, \quad (31)$$

$$\hat{\mathbf{f}} = \mathbf{f}(\hat{x}, \hat{\mathbf{y}}), \quad (32)$$

$$a = \cosh\left(\ell \frac{\|\hat{\mathbf{f}}\|}{\|\hat{\mathbf{y}}\|}\right), \quad (33)$$

$$b = \sinh\left(\ell \frac{\|\hat{\mathbf{f}}\|}{\|\hat{\mathbf{y}}\|}\right). \quad (34)$$

Here, we use  $\mathbf{y}^0 = (\mathbf{y}_1(0), \mathbf{y}_2(0))$  and  $\mathbf{y}^\ell = (\mathbf{y}_1(\ell), \mathbf{y}_2(\ell))$  through a suitable weighting factor  $r$  to calculate  $\mathbf{G}$ , where  $r \in (0, 1)$  is a parameter and  $\hat{x} = r\ell$ . The above method has applied a generalized mid-point rule on the calculation of  $\mathbf{G}$ , and the resultant is a single-parameter Lie group element denoted by  $\mathbf{G}(r)$ .

Throughout this paper we use the superscripted symbol  $\mathbf{y}^0$  to denote the value of  $\mathbf{y}$  at  $x = 0$ , and  $\mathbf{y}^\ell$  the value of  $\mathbf{y}$  at  $x = \ell$ .

### 3.4 A Lie group mapping between two points on the cone

Let us define a new vector

$$\mathbf{F} := \frac{\hat{\mathbf{f}}}{\|\hat{\mathbf{y}}\|}, \quad (35)$$

such that Eqs. (30), (33) and (34) can be also expressed as

$$\mathbf{G} = \begin{bmatrix} \mathbf{I}_{2n-2} + \frac{a-1}{\|\mathbf{F}\|^2} \mathbf{F}\mathbf{F}^t & \frac{b\mathbf{F}}{\|\mathbf{F}\|} \\ \frac{b\mathbf{F}^t}{\|\mathbf{F}\|} & a \end{bmatrix}, \quad (36)$$

$$a = \cosh[\ell\|\mathbf{F}\|], \quad (37)$$

$$b = \sinh[\ell\|\mathbf{F}\|]. \quad (38)$$

From Eqs. (29) and (36) it follows that

$$\mathbf{y}^\ell = \mathbf{y}^0 + \eta\mathbf{F}, \quad (39)$$

$$\|\mathbf{y}^\ell\| = a\|\mathbf{y}^0\| + b \frac{\mathbf{F} \cdot \mathbf{y}^0}{\|\mathbf{F}\|}, \quad (40)$$

where

$$\eta := \frac{(a-1)\mathbf{F} \cdot \mathbf{y}^0 + b\|\mathbf{y}^0\|\|\mathbf{F}\|}{\|\mathbf{F}\|^2}. \quad (41)$$

Substituting  $\mathbf{F}$  in Eq. (39) written as

$$\mathbf{F} = \frac{1}{\eta}(\mathbf{y}^\ell - \mathbf{y}^0) \quad (42)$$

into Eq. (40) and dividing both the sides by  $\|\mathbf{y}^0\|$ , we obtain

$$\frac{\|\mathbf{y}^\ell\|}{\|\mathbf{y}^0\|} = a + b \frac{(\mathbf{y}^\ell - \mathbf{y}^0) \cdot \mathbf{y}^0}{\|\mathbf{y}^\ell - \mathbf{y}^0\|\|\mathbf{y}^0\|}, \quad (43)$$

where, by inserting Eq. (42) for  $\mathbf{F}$  into Eqs. (37) and (38),  $a$  and  $b$  are now written as

$$a = \cosh\left(\frac{\ell\|\mathbf{y}^\ell - \mathbf{y}^0\|}{\eta}\right), \quad (44)$$

$$b = \sinh\left(\frac{\ell\|\mathbf{y}^\ell - \mathbf{y}^0\|}{\eta}\right). \quad (45)$$

Let

$$\cos \theta := \frac{[\mathbf{y}^\ell - \mathbf{y}^0] \cdot \mathbf{y}^0}{\|\mathbf{y}^\ell - \mathbf{y}^0\|\|\mathbf{y}^0\|}, \quad (46)$$

$$\ell_y := \ell\|\mathbf{y}^\ell - \mathbf{y}^0\|, \quad (47)$$

where  $\theta$  is the intersection angle between vectors  $\mathbf{y}^\ell - \mathbf{y}^0$  and  $\mathbf{y}^0$ , and thus from Eqs. (43)-(45) it follows that

$$\frac{\|\mathbf{y}^\ell\|}{\|\mathbf{y}^0\|} = \cosh\left(\frac{\ell_y}{\eta}\right) + \cos \theta \sinh\left(\frac{\ell_y}{\eta}\right). \quad (48)$$

By defining

$$Z := \exp\left(\frac{\ell_y}{\eta}\right), \quad (49)$$

from Eq. (48) we obtain a quadratic equation for  $Z$ :

$$(1 + \cos \theta)Z^2 - \frac{2\|\mathbf{y}^\ell\|}{\|\mathbf{y}^0\|}Z + 1 - \cos \theta = 0. \quad (50)$$

On the other hand, by inserting Eq. (42) for  $\mathbf{F}$  into Eq. (41) we obtain

$$\begin{aligned} \|\mathbf{y}^\ell - \mathbf{y}^0\|^2 = \\ (a-1)(\mathbf{y}^\ell - \mathbf{y}^0) \cdot \mathbf{y}^0 + b\|\mathbf{y}^0\|\|\mathbf{y}^\ell - \mathbf{y}^0\|. \end{aligned} \quad (51)$$

Dividing both sides by  $\|\mathbf{y}^0\|\|\mathbf{y}^\ell - \mathbf{y}^0\|$  and using Eqs. (44)-(47) and (49) we obtain another quadratic equation for  $Z$ :

$$\begin{aligned} (1 + \cos \theta)Z^2 - 2\left(\cos \theta + \frac{\|\mathbf{y}^\ell - \mathbf{y}^0\|}{\|\mathbf{y}^0\|}\right)Z \\ + \cos \theta - 1 = 0. \end{aligned} \quad (52)$$

From Eqs. (50) and (52), the solution of  $Z$  is found to be

$$Z = \frac{(\cos \theta - 1) \|\mathbf{y}^0\|}{\cos \theta \|\mathbf{y}^0\| + \|\mathbf{y}^\ell - \mathbf{y}^0\| - \|\mathbf{y}^\ell\|}, \quad (53)$$

and then from Eqs. (49) and (47) we obtain

$$\eta = \frac{\ell \|\mathbf{y}^\ell - \mathbf{y}^0\|}{\ln Z}. \quad (54)$$

Therefore, we come to an important result that between any two points  $(\mathbf{y}^0, \|\mathbf{y}^0\|)$  and  $(\mathbf{y}^\ell, \|\mathbf{y}^\ell\|)$  on the cone, there exists a Lie group element  $\mathbf{G} \in SO_o(2n-2, 1)$  mapping  $(\mathbf{y}^0, \|\mathbf{y}^0\|)$  onto  $(\mathbf{y}^\ell, \|\mathbf{y}^\ell\|)$ , which is given by

$$\begin{bmatrix} \mathbf{y}^\ell \\ \|\mathbf{y}^\ell\| \end{bmatrix} = \mathbf{G} \begin{bmatrix} \mathbf{y}^0 \\ \|\mathbf{y}^0\| \end{bmatrix}, \quad (55)$$

where  $\mathbf{G}$  is uniquely determined by  $\mathbf{y}^0$  and  $\mathbf{y}^\ell$  through the following equations:

$$\mathbf{G}(\mathbf{y}^0, \mathbf{y}^\ell) = \begin{bmatrix} \mathbf{I}_{2n-2} + \frac{a-1}{\|\mathbf{F}\|^2} \mathbf{F}\mathbf{F}^t & \frac{b\mathbf{F}}{\|\mathbf{F}\|} \\ \frac{b\mathbf{F}^t}{\|\mathbf{F}\|} & a \end{bmatrix}, \quad (56)$$

$$a = \cosh[\ell \|\mathbf{F}\|], \quad (57)$$

$$b = \sinh[\ell \|\mathbf{F}\|], \quad (58)$$

$$\mathbf{F} = \frac{1}{\eta} (\mathbf{y}^\ell - \mathbf{y}^0). \quad (59)$$

$\eta$  is still calculated by Eq. (54), which in view of Eqs. (53) and (46) is fully determined by  $\mathbf{y}^0$  and  $\mathbf{y}^\ell$ . Note that  $\mathbf{G}$  is independent on  $\ell$ .

It should be stressed that the above  $\mathbf{G}$  is different from the one in Eq. (30). In order to feature its dependence only on  $\mathbf{y}^0$  and  $\mathbf{y}^\ell$ , we write it to be  $\mathbf{G}(\mathbf{y}^0, \mathbf{y}^\ell)$ , which is independent on  $r$ . Conversely,  $\mathbf{G}(r)$  is also a function of  $\mathbf{y}^0$  and  $\mathbf{y}^\ell$ , but its dependence on them is through the vector field  $\mathbf{f}$  and the mean value of  $\hat{\mathbf{y}}$ . However, that two Lie group elements  $\mathbf{G}(r)$  and  $\mathbf{G}(\mathbf{y}^0, \mathbf{y}^\ell)$  are both indispensable in our development of the Lie-group shooting method for the ITSP.

#### 4 The Lie-group shooting method

From Eqs. (13)-(16) it follows that

$$\mathbf{y}'_1 = \mathbf{y}_2, \quad (60)$$

$$\mathbf{y}'_2 = \mathbf{h}(x, \mathbf{y}_1), \quad (61)$$

$$\mathbf{y}_1(0) = \mathbf{y}_1^0, \quad \mathbf{y}_1(\ell) = \mathbf{y}_1^\ell, \quad (62)$$

$$\mathbf{y}_2(0) = \mathbf{y}_2^0, \quad \mathbf{y}_2(\ell) = \mathbf{y}_2^\ell, \quad (63)$$

where  $\mathbf{y}_1^0$  and  $\mathbf{y}_2^\ell$  are known from Eqs. (15) and (16), but  $\mathbf{y}_1^\ell$  and  $\mathbf{y}_2^0$  are unknown.

By using Eq. (19) for  $\mathbf{y}$  we have

$$\mathbf{y}^0 = \begin{bmatrix} \mathbf{y}_1^0 \\ \mathbf{y}_2^0 \end{bmatrix}, \quad \mathbf{y}^\ell = \begin{bmatrix} \mathbf{y}_1^\ell \\ \mathbf{y}_2^\ell \end{bmatrix}, \quad (64)$$

and further inserting them into Eq. (42) yields

$$\mathbf{F} := \begin{bmatrix} \mathbf{F}_1 \\ \mathbf{F}_2 \end{bmatrix} = \frac{1}{\eta} \begin{bmatrix} \mathbf{y}_1^\ell - \mathbf{y}_1^0 \\ \mathbf{y}_2^\ell - \mathbf{y}_2^0 \end{bmatrix}. \quad (65)$$

From Eqs. (54), (53) and (46) by inserting Eq. (64) for  $\mathbf{y}^0$  and  $\mathbf{y}^\ell$  we can obtain  $\cos \theta$ ,  $Z$  and  $\eta$  in terms of  $\mathbf{y}_1^0$ ,  $\mathbf{y}_1^\ell$ ,  $\mathbf{y}_2^0$ , and  $\mathbf{y}_2^\ell$ ; however, for saving space we do not write them out.

Comparing Eq. (65) with Eq. (35) and noting that

$$\hat{\mathbf{y}} := \begin{bmatrix} \hat{\mathbf{y}}_1 \\ \hat{\mathbf{y}}_2 \end{bmatrix} = \begin{bmatrix} r\mathbf{y}_1^0 + (1-r)\mathbf{y}_1^\ell \\ r\mathbf{y}_2^0 + (1-r)\mathbf{y}_2^\ell \end{bmatrix} \quad (66)$$

by Eqs. (31) and (64), we obtain

$$\mathbf{y}_1^\ell = \mathbf{y}_1^0 + \frac{\eta}{\|\hat{\mathbf{y}}\|} \mathbf{y}_2^\ell - \frac{r\eta^2}{\|\hat{\mathbf{y}}\|^2} \hat{\mathbf{h}}, \quad (67)$$

$$\mathbf{y}_2^0 = \mathbf{y}_2^\ell - \frac{\eta}{\|\hat{\mathbf{y}}\|} \hat{\mathbf{h}}, \quad (68)$$

where

$$\begin{aligned} \|\hat{\mathbf{y}}\| &= \sqrt{\|\hat{\mathbf{y}}_1\|^2 + \|\hat{\mathbf{y}}_2\|^2} \\ &= \sqrt{\|r\mathbf{y}_1^0 + (1-r)\mathbf{y}_1^\ell\|^2 + \|r\mathbf{y}_2^0 + (1-r)\mathbf{y}_2^\ell\|^2}, \end{aligned} \quad (69)$$

$$\hat{\mathbf{h}} = \mathbf{h}(r\ell, \hat{\mathbf{y}}_1). \quad (70)$$

The above derivation of the governing equations (67) and (68) is obtained by letting the two  $\mathbf{F}$ 's in Eqs. (35) and (59) be equal, which in terms of the Lie group elements  $\mathbf{G}(r)$  and  $\mathbf{G}(\mathbf{y}^0, \mathbf{y}^\ell)$  is essentially identical to the specification of  $\mathbf{G}(r) = \mathbf{G}(\mathbf{y}^0, \mathbf{y}^\ell)$ .

For a specified  $r$ , Eqs. (67) and (68) can be used to generate the new  $(\mathbf{y}_1^\ell, \mathbf{y}_2^0)$  by repeating the above process until  $(\mathbf{y}_1^\ell, \mathbf{y}_2^0)$  converges according to a given stopping criterion:

$$\sqrt{\|\mathbf{y}_{1,i+1}^\ell - \mathbf{y}_{1,i}^\ell\|^2 + \|\mathbf{y}_{2,i+1}^0 - \mathbf{y}_{2,i}^0\|^2} \leq \varepsilon, \quad (71)$$

which means that the norm of the difference between the  $i+1$ -th and the  $i$ -th iterations of  $(\mathbf{y}_1^\ell, \mathbf{y}_2^0)$  is smaller than a given stopping criterion  $\varepsilon$ . If  $\mathbf{y}_2^0$  is available, we can return to Eqs. (13) and (14) and integrate them to obtain  $\mathbf{y}_2(\ell)$ . The above process can be done for all  $r$  in the interval of  $r \in (0, 1)$ . Among these solutions we can pick up the best  $r$ , which leads to the smallest error of

$$\min_{r \in (0,1)} \|\mathbf{y}_2(\ell) - \mathbf{y}_2^\ell\|, \quad (72)$$

since  $\mathbf{y}_2^\ell$  is our target value at the right-boundary specified by Eq. (16).

When the best  $r$  is chosen, from Eq. (68) we can simultaneously calculate the left-boundary conditions of  $v^i$ ,  $i = 2, \dots, n$ , which together with the known left-boundary conditions of  $u^i$ ,  $i = 2, \dots, n$  given in Eq. (15) leading to a complete set of the left-boundary conditions for Eqs. (13) and (14). Then, we can apply any available integrating methods for ODEs, for example, the GPS or the fourth-order Runge-Kutta method (RK4) to calculate  $u$  and  $v$  in the  $x$  domain, and then supplemented with a previously calculated  $T$  we can calculate stress by

$$\sigma(x, t) = \frac{2G}{1-2\nu} [(1-\nu)v(x, t) - (1+\nu)\alpha_t T(x, t)]. \quad (73)$$

## 5 Numerical examples of ITSP

Now, we are ready to apply the LGSM on the calculations of ITSP through the tests of numerical examples. When the input measured temperature data  $T(x_m, t)$  are contaminated by random noise, we can investigate the stability of LGSM by adding different levels of random noise on the measured data:

$$\hat{T}(x_m, t_i) = T(x_m, t_i) + sR(i), \quad (74)$$

where  $T(x_m, t_i)$  is the exact data, and  $s$  specifies the level of noise. We use the function RANDOM\_NUMBER given in Fortran to generate the  $R(i)$ , which are random numbers in  $[-1, 1]$ . Then, the noisy data  $\hat{T}(x_m, t_i)$  are used as inputs in the calculations.

### 5.1 Example 1

Let us first consider a simple ITSP with a closed-form solution of  $T(x, t)$ :

$$T(x, t) = 2\alpha t + x^2, \quad (75)$$

with the boundary conditions

$$T_x(0, t) = 0, \quad T(1, t) = 1 + 2\alpha t, \quad (76)$$

and the initial condition

$$T(x, 0) = x^2. \quad (77)$$

The exact data at  $x_m$  is given by

$$T(x_m, t) = 2\alpha t + x_m^2. \quad (78)$$

In order to compare our numerical results with exact solutions, we also require to derive an exact solution of  $u(x, t)$ , which satisfies

$$u_{tt}(x, t) - c^2 u_{xx}(x, t) = -2kc^2 x, \quad (79)$$

$$0 < x < 1, \quad 0 < t \leq t_f,$$

$$u(x, 0) = b_0 x^3, \quad 0 \leq x \leq 1, \quad (80)$$

$$u_t(x, 0) = a_0 x, \quad 0 \leq x \leq 1, \quad (81)$$

$$u(0, t) = 0, \quad 0 \leq t \leq t_f, \quad (82)$$

$$u_x(1, t) = k(1 + 2\alpha t), \quad 0 \leq t \leq t_f, \quad (83)$$

where

$$a_0 = 2k\alpha, \quad b_0 = \frac{k}{3}. \quad (84)$$

The exact solutions of  $u(x, t)$  and  $\sigma(x, t)$  are found to be

$$u(x, t) = a_0 x t + b_0 x^3, \quad (85)$$

$$\begin{aligned} \sigma(x, t) = & \frac{2G}{1-2\nu} [(1-\nu)(a_0 t + 3b_0 x^2) \\ & - \alpha_t(1+\nu)(2\alpha t + x^2)] \\ & = 0. \end{aligned} \quad (86)$$

The material parameters used here come from the work of Grysa, Cialkowski and Kaminski (1981), which will be fixed to  $\ell = 1$  cm,  $G = 7.9461 \times 10^6$  N·cm<sup>-2</sup>,  $\rho = 7.8$  g·cm<sup>-3</sup>,  $\nu = 0.3$ ,  $\alpha_t = 1.2 \times 10^{-7}$  deg<sup>-1</sup> and  $\alpha = 0.119$  cm<sup>2</sup>·s<sup>-1</sup>. Then  $c$  and  $k$  can be calculated by Eq. (4). In addition these we can compute the other constants by Eq. (84). The final time is fixed to be  $t_f = 2$  s for this example.

Before employing the numerical method of LGSM to calculate this example we use it to demonstrate how to pick up the best  $r$  as specified by Eq. (72). We plot the error of mis-matching the target with respect to  $r$  in Fig. 2. It can be seen that there is a minimum point. Under this  $r$  the left-boundary condition derived from the LGSM provides a numerical solution to best match the right-boundary condition, and then we use the given  $\mathbf{y}_1^0$  and the estimated  $\mathbf{y}_2^0$  to calculate the whole displacement and stress in the rod. In the calculation we were fixed  $\Delta t = 0.005$  s and the stopping criterion  $\varepsilon = 10^{-10}$  was used in Eq. (71).

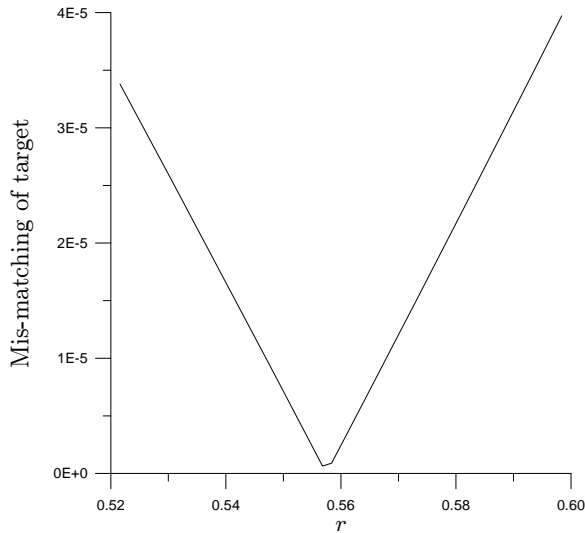


Figure 2: For Example 1 we plot the error of mis-matching the target with respect to  $r$  in a finer interval.

In Fig. 3(a) we compare the computed  $u(x, t_0)$  with the exact one in Eq. (85) at  $t_0 = 0.5$  s, where we use the fourth-order Runge-Kutta method (RK4) with a step size  $\Delta x = 0.005$  to calculate the numerical solution. It can be seen that these

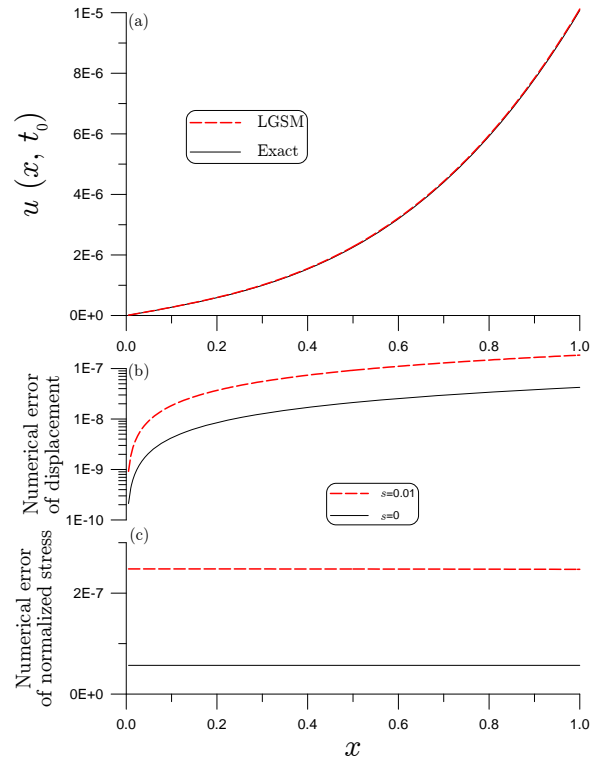


Figure 3: For Example 1: (a) comparing the LGSM and exact solutions of displacement at  $t = t_0$ , (b) displaying the numerical errors of displacement, and (c) displaying the numerical errors of normalized stress.

two curves are almost coincident. Therefore, we plot the numerical error in Fig. 3(b), which is smaller than  $8 \times 10^{-8}$ . Similarly, in Fig. 3(c) we plot the numerical error of the normalized stress  $\sigma/E$ , where  $E$  is the Youngs modulus. The error is smaller than  $10^{-7}$ . It can be seen that our numerical method of LGSM can be applied to the ITSP.

In the above computation we do not consider the noise disturbance on the measured data. When the measured data  $T(x_m, t)$  is polluted by noise, the exact temperature field is naturally contaminated by that disturbance. Hence, by replacing Eq. (16) we consider

$$v^i(\ell) = k[T(\ell, t_i) + sR(i)], \quad i = 2, \dots, n. \quad (87)$$

For the noised case with  $s = 0.01$ , we plot the numerical errors of displacement and normalized

stress in Figs. 3(b) and 3(c). It can be seen that the noise makes the numerical errors slightly larger than these without considering noise. However, the numerical errors are still small and the numerical solutions are acceptable.

## 5.2 Example 2

Suppose that  $f(x) = 0$ , and then by using the classical method we may obtain

$$T(x, t) = \frac{1}{x_m^2} \sum_{j=0}^{\infty} \exp\left(\frac{-\alpha(2j+1)^2\pi^2 t}{4x_m^2}\right) \cos\left(\frac{(2j+1)\pi x}{2x_m}\right) (2j+1)\alpha\pi(-1)^j \int_0^t \exp\left(\frac{\alpha(2j+1)^2\pi^2 \tau}{4x_m^2}\right) F_m(\tau) d\tau. \quad (88)$$

Next, the measured temperature history at  $x_m$  is assumed to be

$$T(x_m, t) = F_m(t) = A_0 \sin \omega t. \quad (89)$$

Then, substituting it into Eq. (88) we can get

$$T(x, t) = \frac{1}{x_m^2} \sum_{j=0}^{\infty} \frac{A_0}{\left(\frac{\alpha(2j+1)^2\pi^2}{4x_m^2}\right)^2 + \omega^2} \cos\left(\frac{(2j+1)\pi x}{2x_m}\right) (2j+1)\alpha\pi(-1)^j \left[ \omega \exp\left(\frac{-\alpha(2j+1)^2\pi^2 t}{4x_m^2}\right) + \frac{\alpha(2j+1)^2\pi^2}{4x_m^2} \sin \omega t - \omega \cos \omega t \right]. \quad (90)$$

For this example we use  $A_0 = 2$ ,  $\omega = 1$  and the temperature measurement is made at  $x_m = 0.8$  cm. The final time is fixed to be  $t_f = 1$  s. In the calculation  $\Delta t = 0.01$  s and  $\Delta x = 1/150$  cm were used. In Fig. 4(a) we plot the mis-matching of target with respect to  $r$  in a finer interval of  $r \in (0.5, 0.65)$ . For this example we have no closed-form solution of stress being compared, and thus we assess the accuracy of our method by testing its matching with the boundary condition  $\sigma(\ell, t) = 0$  in Eq. (7), which is plotted with respect to  $t$  in Fig. 4(b). The maximum error is

smaller than  $9 \times 10^{-6}$ . In Figs. 4(c) and 4(d) we display the displacement and stress at  $t_0 = 0.5$  s along the spatial coordinate.

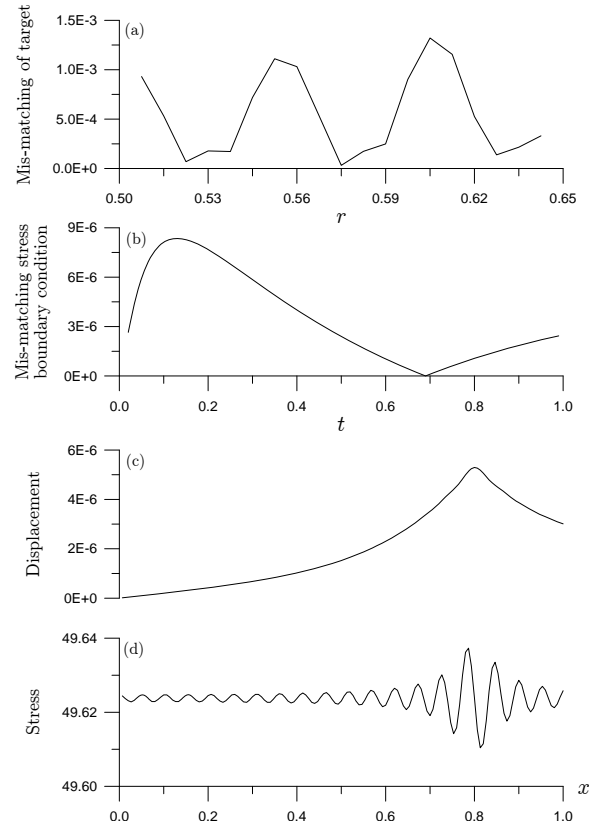


Figure 4: For Example 2: (a) plotting the error of mis-matching the target with respect to  $r$  in a finer interval, (b) plotting the error of mis-matching the stress boundary condition, (c) displaying the LGSM solution of displacement at  $t = t_0$ , and (d) displaying the LGSM solution of stress at  $t = t_0$ .

## 6 The LGSM for heat conduction equation

### 6.1 The LGSM

Under a given left-boundary Neumann condition, a measured temperature  $T(x_m, t)$  and an initial condition, usually we may not have an analytical solution, or its solution is rather complex as the case in Eq. (90) for the previous example. The series form solution may expend much computational time to calculate it. Therefore, as that done

by Chang, Liu and Chang (2005) we consider the following discretizations of Eq. (5):

$$\frac{\partial T^i(x)}{\partial x} = S^i(x), \quad i = 1, \dots, n, \quad (91)$$

$$\frac{\partial S^i(x)}{\partial x} = \frac{T^{i+1}(x) - T^{i-1}(x)}{2\alpha\Delta t}, \quad i = 1, \dots, n-1, \quad (92)$$

$$\frac{\partial S^n(x)}{\partial x} = \frac{T^n(x) - T^{n-1}(x)}{\alpha\Delta t}, \quad (93)$$

where  $T^i(x) = T(x, (i-1)\Delta t)$  and  $S^i(x) = S(x, (i-1)\Delta t)$ . When the central difference is used in Eq. (92) to increase the accuracy, we should use the backward difference in Eq. (93) at the last time point.

While the initial condition is given by Eq. (8) such that  $T^0(x)$  is available, the two boundary conditions in the interval of  $x \in [0, x_m]$  are specified by

$$S^i(0) = 0, \quad i = 1, \dots, n, \quad (94)$$

$$T^i(x_m) = F_m(t_i), \quad i = 1, \dots, n. \quad (95)$$

If the left-boundary condition of  $T^i$  can be obtained, we can treat Eqs. (91)-(93) as a  $2n$ -dimensional coupled ODEs system, and use the GPS or other available numerical integrators to calculate  $T^i$  and  $S^i$ . And then inserting them into Eqs. (13)-(16) we can calculate the  $u^i$  and  $v^i$  by the LGSM as introduced in Section 4. Similarly, in order to obtain the missing left-boundary conditions of  $T^i$ , we can apply the LGSM for Eqs. (91)-(95). We directly write out the required equations:

$$\mathbf{y}_1^0 = \mathbf{y}_1^{x_m} - \frac{\eta}{\|\hat{\mathbf{y}}\|} \mathbf{y}_2^0 - \frac{(1-r)\eta^2}{\|\hat{\mathbf{y}}\|^2} \hat{\mathbf{h}}, \quad (96)$$

$$\mathbf{y}_2^{x_m} = \mathbf{y}_2^0 + \frac{\eta}{\|\hat{\mathbf{y}}\|} \hat{\mathbf{h}}, \quad (97)$$

where

$$\mathbf{y}_1 := \begin{bmatrix} T^1 \\ \vdots \\ T^n \end{bmatrix}, \quad \mathbf{y}_2 := \begin{bmatrix} S^1 \\ \vdots \\ S^n \end{bmatrix}, \quad (98)$$

$$\mathbf{h} := \begin{bmatrix} \frac{T^2(x) - T^0(x)}{2\alpha\Delta t} \\ \vdots \\ \frac{T^n(x) - T^{n-2}(x)}{2\alpha\Delta t} \\ \frac{T^n(x) - T^{n-1}(x)}{\alpha\Delta t} \end{bmatrix}.$$

The two known values are  $\mathbf{y}_2^0 = \mathbf{0}$  and  $\mathbf{y}_1^{x_m}$ , the latter of which is obtained by the measurement at  $x_m$  specified by Eq. (95). The  $\eta$  is similar to that defined by Eq. (54) but with  $\ell$  replaced by  $x_m$ . At the same time  $\|\hat{\mathbf{y}}\|$  and  $\hat{\mathbf{h}}$  are also defined by Eqs. (69) and (70) with  $\ell$  replaced by  $x_m$  and with the above  $\mathbf{y}_1$ ,  $\mathbf{y}_2$  and  $\mathbf{h}$ .

For a specified  $r$ , Eqs. (96) and (97) can be used to generate the new  $(\mathbf{y}_1^0, \mathbf{y}_2^{x_m})$  until they converge according to a given stopping criterion:

$$\sqrt{\|\mathbf{y}_{1,i+1}^0 - \mathbf{y}_{1,i}^0\|^2 + \|\mathbf{y}_{2,i+1}^{x_m} - \mathbf{y}_{2,i}^{x_m}\|^2} \leq \varepsilon. \quad (99)$$

If  $\mathbf{y}_1^0$  is available, we can return to Eqs. (91)-(93) and integrate them to obtain  $\mathbf{y}_1(x_m)$ . The above process can be done for all  $r$  in the interval of  $r \in (0, 1)$ . Among these solutions we may pick up the best  $r$ , which leads to the smallest error of

$$\min_{r \in (0,1)} \|\mathbf{y}_1(x_m) - \mathbf{y}_1^{x_m}\|, \quad (100)$$

since  $\mathbf{y}_1^{x_m}$  is our target value at  $x = x_m$ , wherein we have made a measurement of the temperature history.

## 6.2 Example 3

In order to test the numerical method in Section 6.1 let us consider

$$T(x, t) = \frac{1}{\sqrt{1+4t}} \exp\left(-\frac{x^2}{1+4t}\right). \quad (101)$$

The initial condition is given by  $f(x) = e^{-x^2}$  and the measured temperature history at  $x_m$  is exactly given by

$$T(x_m, t) = \frac{1}{\sqrt{1+4t}} \exp\left(-\frac{x_m^2}{1+4t}\right). \quad (102)$$

For this example we fix the values of parameters to be  $G = 2 \times 10^4 \text{ N}\cdot\text{cm}^{-2}$ ,  $\rho = 2 \text{ g}\cdot\text{cm}^{-3}$ ,  $\nu = 0.3$ ,  $\alpha_t = 10^{-3} \text{ deg}^{-1}$  and  $\alpha = 1 \text{ cm}^2\cdot\text{s}^{-1}$  and  $\ell = 0.5 \text{ cm}$ . The final time is fixed to be  $t_f = 1 \text{ s}$ . In the calculation  $\Delta t = 0.01 \text{ s}$  and  $\Delta x = 1/100 \text{ cm}$  were used.

We first suppose that the temperature measurement is made at  $x_m = 0.1 \text{ cm}$ . In Fig. 5(a) we plot the mis-matching of target with respect to  $r$

in a finer interval of  $r \in (0.45, 0.55)$ . Then, by the LGSM we can determine the unknown left-boundary condition, from which upon comparing with the exact value obtained from Eq. (101) by inserting  $x = 0$  we can calculate the mis-matching error as shown in Fig. 5(b). When both the left-boundary conditions of  $T^i$  and  $S^i$  are known, we can integrate Eqs. (91)-(93) by using the GPS with  $\Delta x = 1/200$  cm towards the right-boundary at  $x = \ell$ . Both the numerical and exact values are plotted in Fig. 5(c), of which it can be seen that these two curves are very close, and thus we plot the numerical error in Fig. 5(d). By comparing Figs. 5(b) and 5(d) the accuracy of boundary conditions is lost one order from  $10^{-4}$  reducing to  $10^{-3}$ . This is due to the numerical integration from the left-side to the right-side.

For this example we have no closed-form solution of stress being compared, and thus we assess the accuracy of our method by testing its matching with the boundary condition  $\sigma(\ell, t) = 0$  in Eq. (7). We plot the mis-matching of the target in Eq. (16) with respect to  $r$  in Fig. 6(a) in a finer interval of  $r \in (0, 10^{-5})$ . We plot the mis-matching of stress boundary condition with respect to  $t$  in Fig. 6(b). The maximum error is smaller than  $5 \times 10^{-4}$ . In Figs. 6(c) and 6(d) we display the displacement and stress at  $t_0 = 0.5$  with respect to the spatial coordinate.

Under the same conditions as that used in the above we use a much smaller  $x_m = 0.01$  in the calculation, of which the results are shown in Figs. 5(b) and 5(d) by the dashed lines. Rather significantly, when  $x_m$  is smaller the present method can produce more accurate boundary conditions. This result indicates that we can measure the temperature far away from the unknown surface boundary condition. In the past works, for example, Grysa, Cialkowsky and Kaminski (1981), in order to obtain a more accurate estimated result, the measurement location must be located near the position of unknown surface boundary condition.

### 6.3 Example 4

In order to compare our numerical results with that obtained by Grysa, Cialkowsky and Kamin-

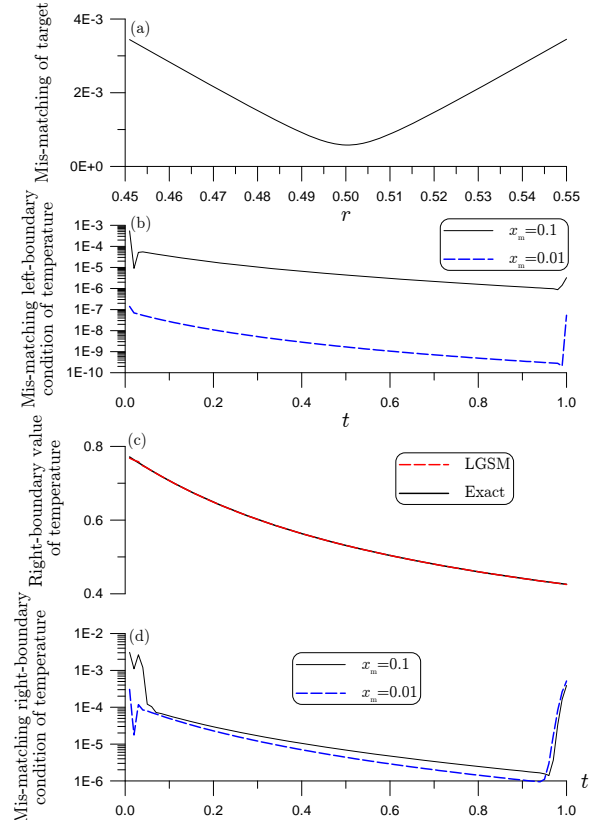


Figure 5: For Example 3: (a) plotting the error of mis-matching the target with respect to  $r$  in a finer interval, (b) plotting the errors of mis-matching the left-boundary condition of temperature for different measurement locations, (c) displaying the LGSM and exact right-boundary temperature, and (d) plotting the errors of mis-matching the right-boundary condition of temperature for different measurement locations.

ski (1981), and Chen, Wu and Hsiao (2004), let us consider a known surface temperature given by  $F_\ell = 1$ . Then the corresponding exactly measured temperature at  $x_m$  can be obtained by inserting  $x = x_m$  into the following equation:

$$T(x, t) = \sum_{j=0}^{\infty} \frac{4(-1)^j}{(2j+1)\pi} \left[ 1 - \exp\left(\frac{-\alpha(2j+1)^2\pi^2 t}{4\ell^2}\right) \right] \cos\left(\frac{(2j+1)\pi x}{2\ell}\right). \quad (103)$$

In Table 1 we compare our numerical results at

Table 1: For Example 4 the comparisons of  $T(\ell/2, t)$  by different methods with the exact ones

$t$	GCK ( $x_m = 0.4\ell$ )	CWH ( $x_m = 0.0\ell$ )	Present ( $x_m = 0.1\ell$ )	Exact
1	0.2663	0.3075	0.3077	0.3075
2	0.4734	0.4980	0.4983	0.4980
3	0.6090	0.6268	0.6271	0.6268
4	0.7068	0.7218	0.7221	0.7218
5	0.7828	0.7926	0.7929	0.7926
10	0.9499	0.9522	0.9525	0.9522
15	0.9885	0.9890	0.9893	0.9890
20	0.9973	0.9975	0.9978	0.9975

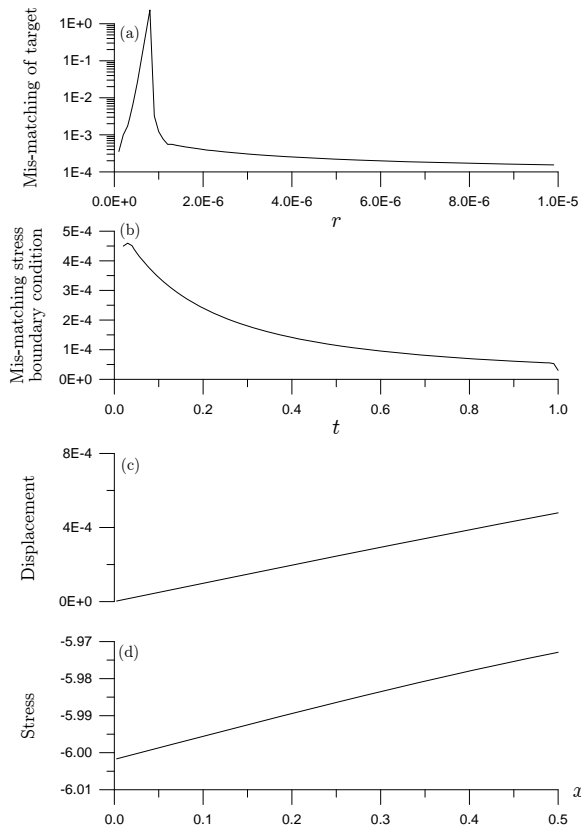


Figure 6: For Example 3: (a) plotting the error of mis-matching the target with respect to  $r$  in a finer interval, (b) plotting the error of mis-matching the stress boundary condition, (c) displaying the LGSM solution of displacement at  $t = t_0$ , and (d) displaying the LGSM solution of stress at  $t = t_0$ .

$x = \ell/2$  but with different times to the results of Grysa, Cialkowsky and Kaminski (1981), and Chen, Wu and Hsiao (2004).

As pointed out by Chen, Wu and Hsiao (2004), the difference between the estimate by Grysa, Cialkowsky and Kaminski (1981) and the exact solution goes up to 13.3%. The present numerical method provides a rather accurate numerical result with the accuracy in the fourth order. In the estimation by Chen, Wu and Hsiao (2004) the measurement is carried out at the left-boundary. If so we can directly apply the RK4 method to integrate the heat conduction equation towards the  $x$  direction. The accuracy may be increased to the same level as that obtained by Chen, Wu and Hsiao (2004).

#### 6.4 Example 5

For this case we consider an unknown surface temperature given by

$$T(\xi = 1, t^*) = t^* + \sin t^* + \cos t^*, \quad (104)$$

where  $\xi = x/\ell$  and  $t^* = \alpha t/\ell^2$  are dimensionless spatial and temporal coordinates. In terms of these coordinates, Eq. (5) can be written as

$$\frac{\partial^2 T(\xi, t^*)}{\partial \xi^2} = \frac{\partial T(\xi, t^*)}{\partial t^*}, \quad 0 < \xi < 1, \quad 0 < t^* \leq t_f^*. \quad (105)$$

Corresponding to the above surface temperature the exactly measured temperature at  $\xi_m$  can be obtained by inserting  $\xi = \xi_m$  into the following

equation:

$$T(\xi, t^*) = \sum_{j=0}^{\infty} (2j+1)\pi(-1)^j \left\{ \frac{1}{a_j^2+1} [(1-a_j)\exp(-a_j t^*) + (1+a_j)\sin t^* - (1-a_j)\cos t^*] + \frac{t^*}{a_j} - \frac{1}{a_j^2} + \frac{1}{a_j} \exp(-a_j t^*) \right\} \cos \frac{(2j+1)\pi\xi}{2}, \quad (106)$$

where

$$a_j := \frac{(2j+1)^2\pi^2}{4}. \quad (107)$$

We calculate this example by the LGSM in Section 6.1 with  $\xi_m = 0.001$  very near the left-boundary. As shown in Fig. 7(a) the recovering curve of the unknown boundary function is coincident with the exact one given in Eq. (104) in the interval of  $0 < t^* < 13$ . Therefore, we plot the numerical error in Fig. 7(b), from which it can be seen that the error is in the order of  $10^{-3}$ . Even for the case with a large noise  $s = 0.02$ , the numerical solution is also acceptable as shown in Fig. 7(a) by the dashed-dotted line.

## 7 Concluding remarks

The inverse thermal stress problems are formulated with a semi-discretization version from the use of temporal finite difference. In order to evaluate the missing boundary conditions for the unknown surface boundary values problems of the ITSP, we have employed the Lie-group shooting method towards the spatial direction to derive the algebraic equations. Hence, we can solve them through a minimum discrepancy solution in a compact space of  $r \in (0, 1)$ . Several numerical examples of the ITSP were examined to evidence that the new algorithm has a fast convergence speed on the solution of  $r$  in a pre-selected finer range than  $(0, 1)$  by using a minimum norm to fit the target equations, which usually requires only a few number of iterations to select the best  $r$ . The new method is robust against the noise disturbance. Through this study, it can be seen that the new Lie-group shooting method is accurate, effective and stable. Its numerical implementation

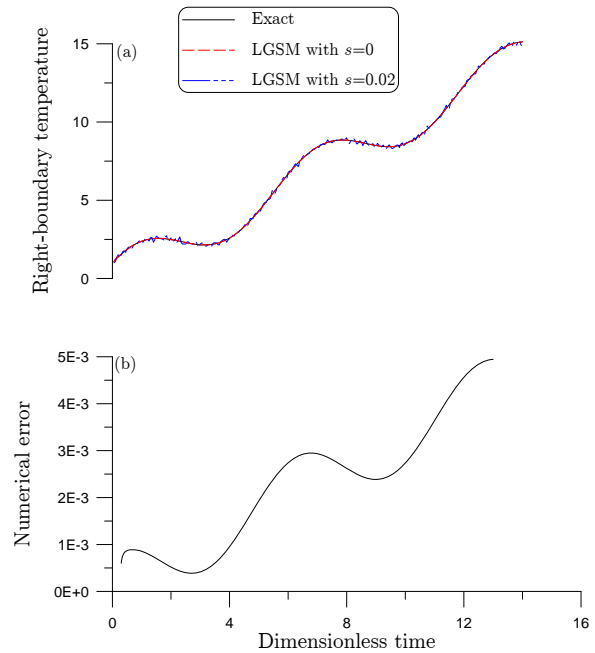


Figure 7: For Example 5: (a) comparing the LGSM and exact right-boundary condition of temperature, and (b) plotting the error of mismatching the right-boundary condition of temperature.

is very simple and the computational speed is very fast. The numerical behavior of LGSM is very unlike that of the conventional numerical methods. It is found that the numerical errors of LGSM are greatly reduced when the measurement locations are more near to the left-boundary. This property is very important, when in a practical use we are usually required to mount a thermocouple as far away from the surface of unknown boundary condition as possible in order to avoid destroying the engineering structure.

**Acknowledgement:** Taiwan's National Science Council project NSC-96-2221-E-019-027-MY3 granted to the author is highly appreciated.

## References

Al-Hunuti, N. S.; Al-Nimr, M. A.; Naji, M. (2001): Dynamic response of a rod due to a moving heat source under the hyperbolic heat conduction model. *J. Sound Vib.*, vol. 242, pp. 629-640.

- Blanc, G.; Raynaud, M.** (1996): Solution of the inverse heat conduction problem from thermal strain measurements. *J. Heat Transfer ASME*, vol. 118, pp. 842-849.
- Chang, C. W.; Chang, J. R.; Liu, C.-S.** (2006): The Lie-group shooting method for boundary layer equations in fluid mechanics. *J. Hydrodynamics*, vol. 18, Issue 3, Supplement 1, pp. 103-108.
- Chang, C. W.; Chang, J. R.; Liu, C.-S.** (2008): The Lie-group shooting method for solving classical Blasius flat-plate problem. *CMC: Computers, Materials & Continua*, in press.
- Chang, C. W.; Liu, C.-S.; Chang, J. R.** (2005): A group preserving scheme for inverse heat conduction problems. *CMES: Computer Modeling in Engineering & Sciences*, vol. 10, pp. 13-38.
- Chang, J. R.; Liu, C.-S.; Chang, C. W.** (2007a): A new shooting method for quasi-boundary regularization of backward heat conduction problems. *Int. J. Heat Mass Transfer*, vol. 50, pp. 2325-2332.
- Chang, C. W.; Liu, C.-S.; Chang, J. R.** (2007b): The Lie-group shooting method for quasi-boundary regularization of backward heat conduction problems. *ICCES on line Journal*, vol. 3, pp. 69-79.
- Chen, H. T.; Chang, S. M.** (1990): Application of the hybrid method to inverse heat conduction problems. *Int. J. Heat Mass Transfer*, vol. 33, pp. 621-628.
- Chen, H. T.; Lin, S. Y.; Fang, L. C.** (2001): Estimation of surface temperature in two-dimensional inverse heat conduction problems. *Int. J. Heat Mass Transfer*, vol. 44, pp. 1455-1463.
- Chen, H. T.; Lin, S. Y.; Fang, L. C.** (2002): Estimation of two-sided boundary conditions for two-dimensional inverse heat conduction problems. *Int. J. Heat Mass Transfer*, vol. 45, pp. 15-23.
- Chen, H. T.; Wu, X. Y.; Hsiao, Y. S.** (2004): Estimation of surface condition from the theory of dynamic thermal stress. *Int. J. Thermal Sci.*, vol. 43, pp. 95-104.
- Chen, X.; Liu, Y.** (2001): Thermal stress analysis of multi-layer thin films and coatings by an advanced boundary element method. *CMES: Computer Modeling in Engineering & Sciences*, vol. 2, pp. 337-350.
- Grysa, K.; Cialkowski, M. L.; Kaminski, H.** (1981): An inverse temperature field problem of the theory of thermal stresses. *Nuclear Engng. Design*, vol. 64, pp. 169-184.
- Gulluoglu, A. N.; Tsai, C. T.** (2000): Effect of growth direction on twin formation in GaAs crystals grown by the vertical gradient freeze method. *CMES: Computer Modeling in Engineering & Sciences*, vol. 1, pp. 85-90.
- Liu, C.-S.** (2001): Cone of non-linear dynamical system and group preserving schemes. *Int. J. Non-Linear Mech.*, vol. 36, pp. 1047-1068.
- Liu, C.-S.** (2004): Group preserving scheme for backward heat conduction problems. *Int. J. Heat Mass Transfer*, vol. 47, pp. 2567-2576.
- Liu, C.-S.** (2006a): The Lie-group shooting method for nonlinear two-point boundary value problems exhibiting multiple solutions. *CMES: Computer Modeling in Engineering & Sciences*, vol. 13, pp. 149-163.
- Liu, C.-S.** (2006b): Efficient shooting methods for the second order ordinary differential equations. *CMES: Computer Modeling in Engineering & Sciences*, vol. 15, pp. 69-86.
- Liu, C.-S.** (2006c): The Lie-group shooting method for singularly perturbed two-point boundary value problems. *CMES: Computer Modeling in Engineering & Sciences*, vol. 15, pp. 179-196.
- Liu, C.-S.** (2006d): An efficient backward group preserving scheme for the backward in time Burgers equation. *CMES: Computer Modeling in Engineering & Sciences*, vol. 12, pp. 55-65.
- Liu, C.-S.** (2006e): One-step GPS for the estimation of temperature-dependent thermal conductivity. *Int. J. Heat Mass Transfer*, vol. 49, pp. 3084-3093.
- Liu, C.-S.** (2006f): An efficient simultaneous estimation of temperature-dependent thermophysical properties. *CMES: Computer Modeling in Engineering & Sciences*, vol. 14, pp. 77-90.
- Liu, C.-S.** (2007): Identification of temperature-dependent thermophysical properties in a partial

differential equation subject to extra final measurement data. *Numer. Meth. Partial Diff. Eq.*, vol. 23, pp. 1083-1109.

**Liu, C.-S.** (2008a): An LGSM to identify non-homogeneous heat conductivity functions by an extra measurement of temperature. *Int. J. Heat Mass Transfer*, vol. 51, pp. 2603-2613.

**Liu, C.-S.** (2008b): An LGEM to identify time-dependent heat conductivity function by an extra measurement of temperature gradient. *CMC: Computers, Materials & Continua*, in press.

**Liu, C.-S.** (2008c): Solving an inverse Sturm-Liouville problem by a Lie-group method. *Boundary Value Problems*, vol. 2008, Article ID 749865.

**Liu, C.-S.; Chang, J. R.** (2008): The Lie-group shooting method for multiple-solutions of Falkner-Skan equation under suction-injection conditions. *Int. J. Non-Linear Mech.*, in press.

**Liu, C.-S.; Chang, C. W.; Chang, J. R.** (2006a): Past cone dynamics and backward group preserving schemes for backward heat conduction problems. *CMES: Computer Modeling in Engineering & Sciences*, vol. 12, pp. 67-81.

**Liu, C.-S.; Chang, C. W.; Chang, J. R.** (2006b): The Lie-group shooting method for steady-state Burgers equation with high Reynolds number. *J. Hydrodynamics*, vol. 18, Issue 3, Supplement 1, pp. 367-372.

**Liu, C.-S.; Liu, L. W.; Hong, H. K.** (2007): Highly accurate computation of spatial-dependent heat conductivity and heat capacity in inverse thermal problem. *CMES: Computer Modeling in Engineering & Sciences*, vol. 17, pp. 1-18.

**Miyazaki, N.; Tamura, T.; Yamamoto, K.** (2000): Cracking of GSO Single Crystal Induced by Thermal Stress. *CMES: Computer Modeling in Engineering & Sciences*, vol. 1, pp. 99-106.